25-29 August 2024
inter.noise
NANTES FRANCE

Introduction of oblique plane waves through a forcing source term in Euler equations

Giovanni Coco[1]
Ecole Centrale de Lyon, CNRS, Universite Claude Bernard Lyon 1, INSA Lyon, LMFA, UMR5509, 69130, Ecully, France and Safran Aircraft Engines, Rond Point René Ravaud-Réau, 77550, Moissy-Cramayel, France

Didier Dragna[2]
Ecole Centrale de Lyon, CNRS, Universite Claude Bernard Lyon 1, INSA Lyon, LMFA, UMR5509, 69130, Ecully

Christophe Bailly[3]
Ecole Centrale de Lyon, CNRS, Universite Claude Bernard Lyon 1, INSA Lyon, LMFA, UMR5509, 69130, Ecully

Hélène Posson[4]
Safran Aircraft Engines, Rond Point René Ravaud-Réau, 77550, Moissy-Cramayel, France

ABSTRACT

The propagation of shock waves generated by a transonic flow at the tip of a propeller blade is numerically calculated in order to determine the pressure footprint on an aircraft fuselage. An academic case is first proposed to validate the methodology. An incoming signal is built up as oblique harmonic plane waves. The signal is introduced in the computational domain using a Gaussian volume forcing term in the conservation of mass and energy equations. The Euler equations are solved in two dimensions using finite-difference schemes with low dispersion and dissipation. Selective filtering has also been integrated in the algorithm to remove grid-to-grid oscillations. The numerical solution is compared to an analytical solution based on the tailored Green function. An illustration for a realistic open rotor is then considered. The pressure signal near the blade tip, determined from a preliminary RANS simulation, is introduced using a volume source in a solver of the Euler equations.

1. INTRODUCTION

According to the International Air Transport Association (IATA) report [1], the global economy is growing at a rate of about 3 percent per year. This leads to a tightening of International Civil Aviation Organization (ICAO) regulations [2] to limit the impact of such growth. The development

[1]giovanni.coco@ec-lyon.fr

[2]didier.dragna@ec-lyon.fr

[3]christophe.bailly@ec-lyon.fr

[4]helene.de-laborderie@safrangroup.com

of cutting-edge technologies is therefore crucial to operating in such an environment, such as the use of an open fan that can reduce emissions by 20% [3] compared to conventional architectures. However, given the absence of the nacelle, the propagation of shock-waves generated at the blade tips and their impact on the fuselage should be evaluated.

The generation and propagation of shock-waves has already been addressed in the works of Thisse [4] and Daroukh *et al.* [5] in the case of a classical turbofan, following a CFD/CAA coupling strategy. This strategy involves an initial CFD (Computational Fluid Dynamics) calculation to generate the pressure field around the rotor, and then its propagation by a CAA (Computational Aeroacoustics) calculation. The transition from CFD to CAA is done by a direct introduction of the pressure signal in the computational domain using the method of characteristics. In this study, an alternative method of introducing the pressure signal through a forcing source term inserted into the conservation equations in the case of shock-waves generated by an open fan is proposed.

An academic case with an analytical model for oblique plane wave propagation is proposed in Section 2 to validate the proposed method. Section 3 presents the numerical method implemented in the simulation, the results of which are discussed in Section 4. Finally, in Section 5, the application case with an open fan engine is presented. A summary of the results obtained and possible future work are discussed in Section 6.

2. ANALYTICAL SOLUTION

An analytical solution for the propagation of oblique plane waves inclined by a θ angle is proposed. As demonstrated by Maeda and Colonius [6], the linearized Euler equations in a homogeneous medium at rest can be rewritten as

$$\frac{1}{c_0^2}\frac{\partial^2 p'}{\partial t^2} - \nabla^2 p' = \frac{\partial S_1}{\partial t} - \nabla \cdot \boldsymbol{S_2} \tag{1}$$

$$\frac{\partial \boldsymbol{\omega'}}{\partial t} = \frac{\nabla \times \boldsymbol{S_2}}{\rho_0} \tag{2}$$

$$\rho_0 T_0 \frac{\partial s'}{\partial t} = S_3 - \frac{c_0^2}{\gamma - 1} S_1 \tag{3}$$

where c_0 is the mean speed of sound, p' is the pressure perturbation, t is time, $\boldsymbol{\omega'}$ is the vorticity perturbation, ρ_0 is the mean density, T_0 is the mean temperature, s' is the entropy perturbation, γ is the ratio of specific heats and S_1, $\boldsymbol{S_2}$ and S_3 are respectively the mass, momentum and energy source terms.

The source term $\boldsymbol{S_2}$ is taken to be zero here. To avoid the introduction of entropy into the system, S_1 and S_3 must be chosen appropriately to cancel the source term in Equation 3, leading to

$$S_3 = \frac{c_0^2}{\gamma - 1} S_1 \tag{4}$$

The source term generating harmonic oblique waves is defined as

$$S_3 = \Lambda_{\rho e} \sin\left[\omega\left(t - \frac{z}{c_0}\sin\theta\right)\right]\delta\left(x - x_s\right) \tag{5}$$

where $\Lambda_{\rho e}$ is the signal amplitude, ω is the angular frequency, x and z are the coordinates along the horizontal and vertical axis respectively, θ is the inclination angle, x_s is the position of the

source along the horizontal axis and $\delta(x-x_s)$ is the Dirac distribution centered on the source plane.

The analytical solution is provided by the convolution between the three-dimensional free space Green's function for the wave equation and the source term $\partial S_1/\partial t$ according to Equation 1. The three-dimensional Green's function is defined as

$$g_0(x,y,z,t) = \frac{1}{4\pi R}\delta(t - R/c_0),$$

where $R = \sqrt{x^2+y^2+z^2}$. The convolution product is recast as follows:

$$\begin{aligned} p(x,y,z,t) &= \left(g_0 * \frac{\partial S_1}{\partial t}\right)_{x,y,z,t} \\ &= \iiiint_{-\infty}^{+\infty} g_0(x-x',y-y',z-z',t-t')\frac{\partial S_1}{\partial t'}(x',y',z',t')dx'dy'dz'dt' \\ &= \iiiint_{-\infty}^{+\infty} \frac{1}{4\pi R'}\delta(t-t'-R'/c_0)\frac{\partial S_1}{\partial t'}(x',y',z',t')dx'dy'dz'dt' \\ &= \iiint_{-\infty}^{+\infty} \frac{1}{4\pi R'}\frac{\partial S_1}{\partial t}(x',y',z',t-R'/c_0)dx'dy'dz' \end{aligned}$$

where $R' = \sqrt{(x-x')^2+(y-y')^2+(z-z')^2}$ is the distance between the source and the observer. Substituting the source term of Equation 5 in the expression above, the exact analytical solution for a two-dimensional domain, taking $y = 0$, reads as

$$p(x,z,t) = \frac{\gamma-1}{2c_0}\frac{\Lambda_{\rho e}}{\cos\theta}\sin\left[\omega t - k_0 z\sin\theta - k_0(x-x_s)\cos\theta\right] \tag{6}$$

with $k_0 = \omega/c_0$ the wave number.

3. NUMERICAL METHOD

An academic test case is proposed to validate the wave introduction method. The two-dimensional Euler equations are solved:

$$\frac{\partial \boldsymbol{U}}{\partial t} + \frac{\partial \boldsymbol{E}}{\partial x} + \frac{\partial \boldsymbol{F}}{\partial z} = \boldsymbol{S}$$

with

$$\boldsymbol{U} = \begin{pmatrix} \rho \\ \rho u \\ \rho v \\ \rho e \end{pmatrix} \quad \boldsymbol{E} = \begin{pmatrix} \rho u \\ \rho u^2 + p \\ \rho uv \\ u(\rho e + p) \end{pmatrix} \quad \boldsymbol{F} = \begin{pmatrix} \rho v \\ \rho uv \\ \rho v^2 + p \\ v(\rho e + p) \end{pmatrix} \quad \boldsymbol{S} = \begin{pmatrix} S_1 \\ 0 \\ 0 \\ S_3 \end{pmatrix}$$

where $\boldsymbol{U}$ is the vector of conservative variables, $\boldsymbol{E}$ and $\boldsymbol{F}$ are the flux vectors, $\boldsymbol{S}$ is the source vector, ρ is density, u and v are the velocities along x and z directions respectively, e is the internal energy per unit volume and p is the pressure.

All the variables are dimensionless and the computational domain is uniform. The chosen mesh spacing is $\Delta x = 0.1$, the speed of sound is $c_0 = 1$ and the CFL number is fixed at 0.5. The spatial derivation is performed by an eleven-point centered finite difference numerical scheme developed by Bogey and Bailly [7] that minimizes the dispersion and dissipation error. In addition, an eleven-point selective filter is used to eliminate grid-to-grid oscillations, as these can induce numerical instabilities. Temporal integration is performed with a six-step fourth-order explicit

Runge-Kutta scheme developed by Berland *et al.* [8] using only two storage locations per variable.

The sources are distributed along a vertical line set at $x = x_s$. The signal introduced is an oblique plane wave defined as

$$S_3 = \Lambda_{\rho e} \sin(\omega t - k_0 z \sin\theta)\, \beta(x - x_s)$$

according to Equation 5, where β is a Gaussian distribution centered on the source line and defined as

$$\beta(x) = \frac{\exp\left[-\log 2 \frac{x^2}{b^2}\right]}{\sqrt{\frac{\pi}{\log 2} b}}$$

The sketch presented in Figure 1 shows the boundary conditions imposed in the computational domain. Periodic conditions are applied on the upper and lower edges. This choice was made to allow the propagation of oblique waves throughout the domain. Non-reflection conditions are applied on the left and right edges through the method of characteristics developed by Thompson ([9], [10]). A strong dissipation zone is also implemented on the first 30 points near these same edges via the Perfectly Matched Layer (PML) technique developed by Hu [11]. This is because the method of characteristics is purely one-dimensional, and its effectiveness is reduced in the presence of incident waves whose wave vector is not perpendicular to the edge, as stated by Poinsot and Lele [12].

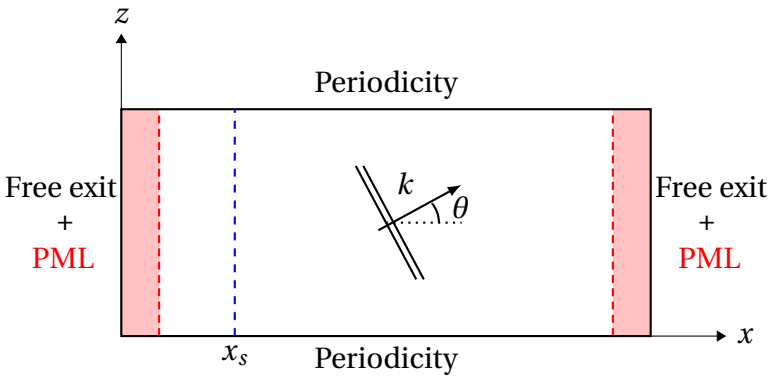

Figure 1: Sketch of the computational domain with boundary conditions. The red zones represent the areas where the PML technique is applied.

4. RESULTS

For this academic case, the choice was made to run all simulations keeping twenty points per wavelength along the x-axis. The input signal is introduced along the line $x_s = 13$. The horizontal length of the domain is $L_x = 40$. The signal is infinitely periodic in the z-direction with n periods along the vertical source line. To introduce an oblique plane wave that meets this condition, the inclination angle θ must be chosen appropriately. It is therefore chosen according to the vertical length L_z of the domain and the wavelength λ_x as per this relation:

$$\theta = \tan^{-1}\left(\frac{\lambda_x n}{L_z}\right) \tag{7}$$

Table 1 shows the parameters chosen for the four simulations. The signal amplitude $\Lambda_{\rho e}$ for Case 4 is halved to reduce nonlinear effects due to the amplification factor.

Case	$\Lambda_{\rho e}$	L_z	θ
1	10^{-3}	10	0°
2	10^{-3}	10	21.8°
3	10^{-3}	5	38.7°
4	$0.5 \cdot 10^{-3}$	2	63.4°

Table 1: Parameters of the simulations.

The results obtained for the academic case are presented for different inclination angles in Figures 2 and 3. As shown in Equation 6, the amplification factor $1/\cos\theta$ is responsible for the increase in signal amplitude.

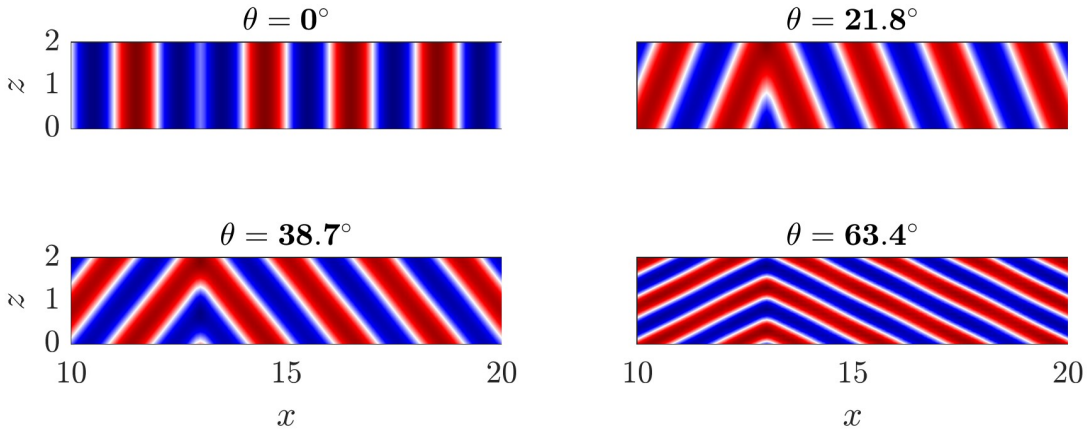

Figure 2: Pressure oscillations fields for different inclination angles θ.

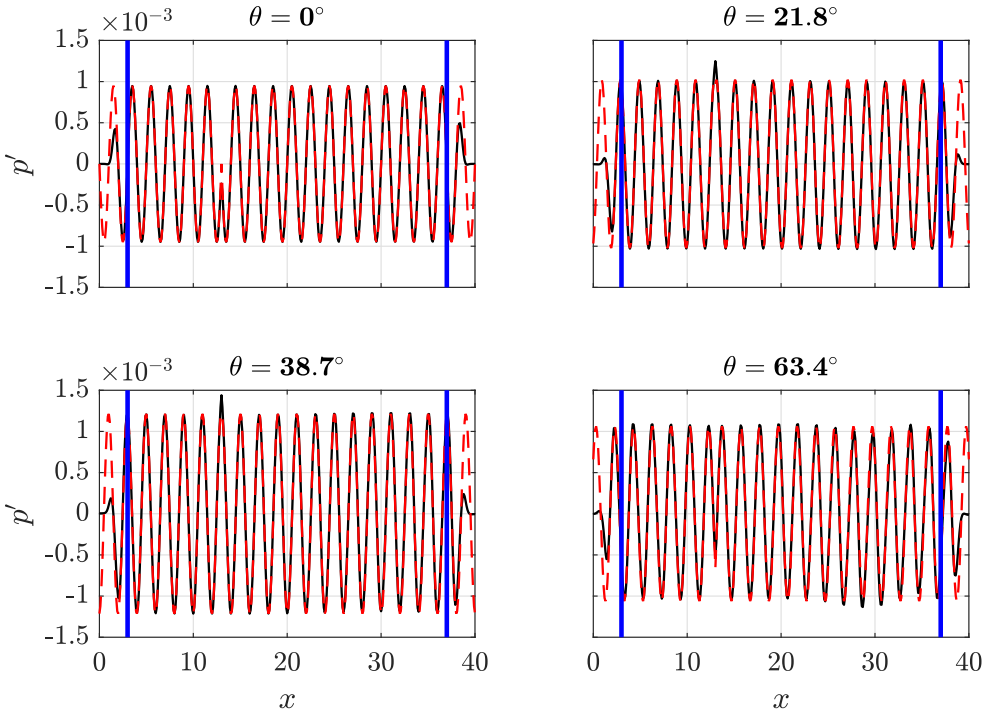

Figure 3: Simulation results (in black solid line) compared with the analytical solution (in red dashed line) for different inclination angles at $z = 1$. Vertical blue solid lines indicate the beginning of the PML regions.

Comparison between the analytical solution and the simulation shows good agreement in Cases 1, 2 and 3. For Case 4, a small inaccuracy is observed for $x > 25$. This effect could be due to the signal introduction method, which is done at the end of each iteration. An improvement could be observed in the case where the introduction occurs at each substep of the Runge-Kutta cycle, as demonstrated by Gloerfelt and Le Garrec [13].

5. APPLICATION CASE

The method of wave introduction by a volumic forcing source term is now tested on a more realistic case. In this case, the source term is the pressure signal generated by the rotation of an open fan of radius R rotating at an angular velocity Ω. This signal corresponds to the pressure field obtained from a RANS simulation, and extracted on a cylindrical surface in the near-field around the engine. Rotor motion at high speed may generate shock waves on the blades. Since this is an open fan architecture, without nacelle and the associated acoustic liner, the shock waves are free to propagate into the environment. Analysis of the propagation of such waves and their impact on the fuselage need to be evaluated.

The sketch in Figure 4 shows the cylindrical surface and the plane in which the signal is propagated. The azimuthal spacing around the surface is Δs and the mesh spacing in the simulation plane is $\Delta x = \Delta z$. The source term is introduced along the line of intersection between the cylindrical surface and the simulation plane.

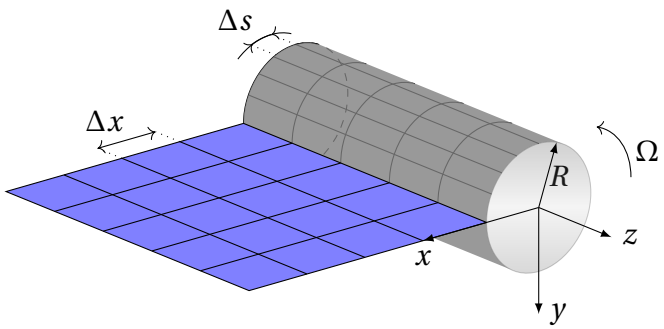

Figure 4: Sketch for the application case. The blue xz plane corresponds to the simulation domain. The pressure signal is introduced in the line of intersection between the plane and the cylindrical surface.

In the case of a rotor, it is important to tie the angular velocity to the simulation parameters, as it is closely related to the introduction of the pressure signal. The time step Δt is actually related to both rotational speed Ω and CFL according to the following relations:

$$\Delta t = \frac{\Delta s}{R\Omega} \tag{8}$$

$$\Delta t = \frac{\Delta x \, \mathrm{CFL}}{c_0} \tag{9}$$

Using Equations 8 and 9, an expression can be derived to obtain the adapted Δs for a given Δx:

$$\Delta s = R\Omega \frac{\Delta x \, \mathrm{CFL}}{c_0} \tag{10}$$

An interpolation must be made on the cylinder mesh according to the chosen Δx. This operation allows one at each iteration to introduce into the computational domain the signal

trace corresponding to the rotation of the engine at a given time instant, taking into account the rotational velocity.

The normalized fields of total pressure and pressure oscillations extracted from the cylindrical surface are shown in Figure 5. Pressure fluctuations are calculated from an average of the pressure field along the azimuthal direction. A non-reflective output condition with a PML zone has been set at the left edge. A reflective condition is imposed on the right edge to simulate the presence of the fuselage wall. Periodicity conditions with a PML zone are applied at the top and bottom edges. Since the data are confidential, the parameters chosen for this simulation do not correspond to the real configuration.

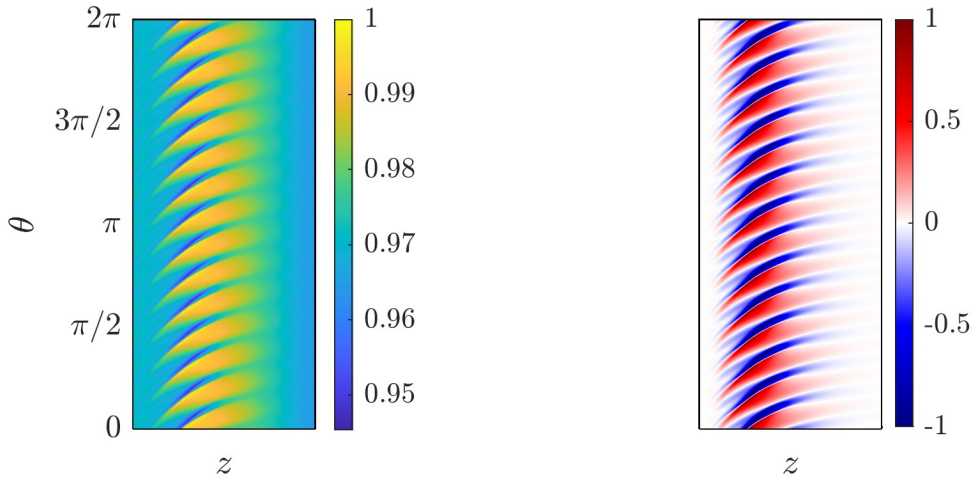

Figure 5: Pressure signal on the cylindrical surface: pressure field on the left, pressure fluctuation field on the right.

The propagation of shock waves in the xz plane is reported in the snapshots in Figure 6. The signal is first introduced along the vertical line at $x = x_s$ (Figure 6a) and propagates to the left and right of it (Figure 6b). Then it is reflected on the wall on the right (Figure 6c) and exits the computational domain on the edge on the left (Figure 6d).

A comparison between the pressure signal extracted from the cylindrical surface and the pressure signal introduced at $x = x_s$ is shown in Figure 7. This is made some iterations before the reflected signal crosses the source line, so that the correct introduction of the source term can be assessed. As seen in Equation 6 for the academic case, an amplification factor based on the angle of inclination of the wavefront should be taken into account. This may explain the slight difference between the source signal extracted from the cylindrical surface and the pressure signal actually introduced into the computational domain.

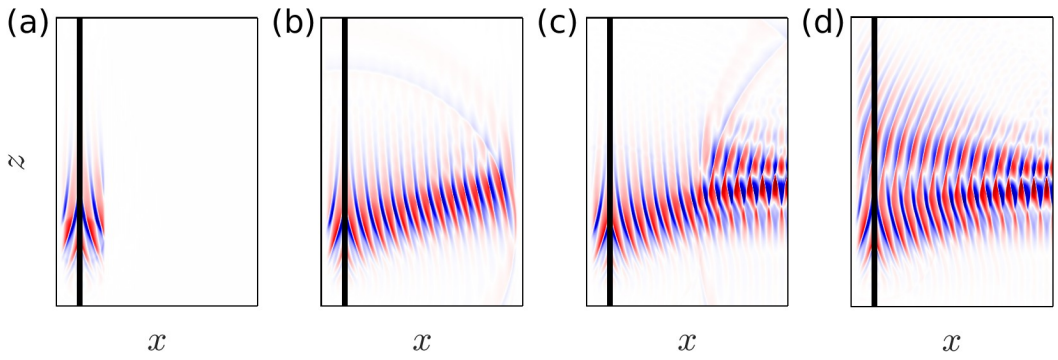

Figure 6: Snapshots of the pressure field. The black vertical solid line corresponds to $x = x_s$.

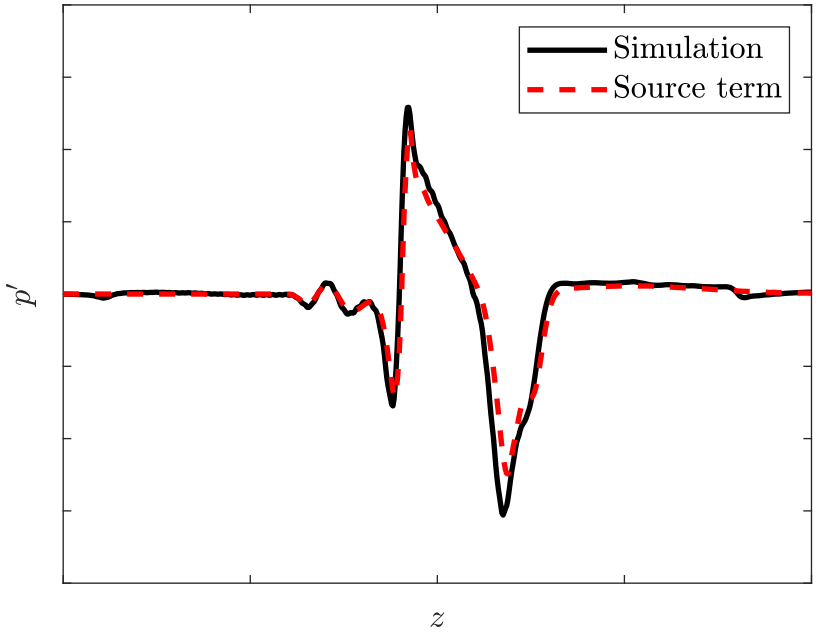

Figure 7: Comparison between the theoretical source term and the actual source term introduced in the simulation at $x = x_s$.

6. CONCLUSION

The method presented in this study to introduce a given signal in a computational domain is easy to implement in a solver for Euler equations. The results obtained in the academic case of oblique plane waves show good agreement with the analytical solution, taking into account the amplification term as the angle of inclination of the waves increases. The case of application to an open fan engine needs further analysis and investigation, such as including a mean flow and comparing the results with the Ffowcs Williams-Hawkings integral method. In perspective, a three dimensional simulation of the input signal of the cylindrical surface is to be carried out for a signal analysis on the fuselage.

ACKNOWLEDGEMENTS

This work was performed within the framework of the industrial chair ARENA (ANR-18-CHIN-0004-01) co-financed by Safran Aircraft Engines and the French National Research Agency (ANR),

and within the framework of the LABEX CeLyA (ANR-10-LABX-0060) of Université de Lyon, within the program « Investissements d'Avenir » (ANR-16-IDEX-0005) operated by the French National Research Agency (ANR).

REFERENCES

1. International Air Transport Association (IATA). Global Outlook for Air Transport: Highly Resilient, Less Robust, 2023.
2. International Civil Aviation Organization (ICAO). Annex 16 - Environmental Protection - Volume I - Aircraft Noise, 2017.
3. CFM RISE Program: Revolutionary Innovation for Sustainable Engines. Technical report, 2023.
4. Johan Thisse. *Prévision du bruit d'onde de choc d'un turboréacteur en régime transsonique par des méthodes analytiques et numériques*. PhD thesis, Ecole nationale supérieure d'arts et métiers - ENSAM, 2015.
5. Majd Daroukh, Cyril Polacsek, and Alain Chelius. Shock Wave Generation and Radiation from a Turbofan Engine Under Flow Distortion. *AIAA Journal*, 58(2):787, 2019.
6. Kazuki Maeda and Tim Colonius. A source term approach for generation of one-way acoustic waves in the Euler and Navier–Stokes equations. *Wave Motion*, 75:36–49, 2017.
7. Christophe Bogey and Christophe Bailly. A family of low dispersive and low dissipative explicit schemes for flow and noise computations. *Journal of Computational Physics*, 194(1):194–214, 2004.
8. Julien Berland, Christophe Bogey, and Christophe Bailly. Low-dissipation and low-dispersion fourth-order Runge–Kutta algorithm. *Computers & Fluids*, 35:1459–1463, 2006.
9. Kevin W Thompson. Time dependent boundary conditions for hyperbolic systems. *Journal of Computational Physics*, 68(1):1–24, 1987.
10. Kevin W Thompson. Time-dependent boundary conditions for hyperbolic systems, II. *Journal of Computational Physics*, 89(2):439–461, 1990.
11. Fang Q Hu. A Stable, Perfectly Matched Layer for Linearized Euler Equations in Unsplit Physical Variables. *Journal of Computational Physics*, 173(2):455–480, 2001.
12. T. J Poinsot and S. K Lele. Boundary conditions for direct simulations of compressible viscous flows. *Journal of Computational Physics*, 101(1):104–129, 1992.
13. Xavier Gloerfelt and Thomas Le Garrec. Generation of inflow turbulence for aeroacoustic applications. In *14th AIAA/CEAS Aeroacoustics Conference*. American Institute of Aeronautics and Astronautics, 2008.